Journal of
NANOSTRUCTURES
JNS
NANOSTRUCTURES
JNS.kashanu.ac.ir

Ultrasound Assisted Synthesis and Characterization of Mn Doped CdS Nanocrystalline Zinc-Blendes

P. Iranmanesh [a,*], S. Saeednia [b], S. Rashidi Dafeh [a], F. Yahyanasab [a]

[a] *Department of physics, Faculty of Science, Vali-e-Asr University of Rafsanjan, Rafsanjan, 77188-97111 Iran.*

[b] *Department of Chemistry, Faculty of Science, Vali-e-Asr University of Rafsanjan, Rafsanjan, 77188-97111 Iran.*

Article history:
Received 01/10/2015
Accepted 19/11/2015
Published online 01/12/2015

Keywords:
Nanoparticles
Mn doped Cadmium Sulfide
Quantum size effect
ultrasonic irradiation

**Corresponding author:*
E-mail address*:*
p.iranmanesh@vru.ac.ir;
p.iranmanesh@gmail.com
aataie@ut.ac.ir
Phone: 98 915 5117584
Fax: +98 34 31312429

Abstract

$Cd_{1-x}Mn_xS$ (x = 0, 0.1, 0.2) nanoparticles, prepared by co-precipitation method under ultrasonic irradiation, were studied by means of X-ray diffraction, scanning electron microscopy, FTIR and UV-Vis spectroscopy measurements. The average particle size of nanoparticles from the scanning electron microscopy image is about 20-30 nm. Results show that partial substitution of Cd by Mn leads to a reduction in lattice parameters and enhancement of band gap energy. This is attributed to the nanometric grain size and quantum confinement effects. The particle size is calculated to be around 2 nm that is almost in agreement with the crystallite size estimated from the XRD result.

1. Introduction

In recent years, special attention has been paid to the fascinating physicochemical properties of nanomaterials (nanoclusters, nanoparticles, nanocrystallites, or nanomaterials) of semiconductors and the wide possibilities of using these properties in practice such as sensors, detectors, electronics, optoelectronics, biology and more [1-11]. The properties of nanomaterials especially nanoparticles strongly depend on the size and shape of the particles, particle size distribution and quantum size effect. At nanoparticle sizes of semiconductor, the energy gap (band gap) increases, and the optical spectrum is shifted toward the short-wavelength region and their some physical properties differ noticeably from those of the corresponding bulk material [1-13]. II-VI semiconductor nanoparticles especially cadmium sulfide (CdS) are nowadays a very interesting topic in both applied and fundamental

physics. Their importance was due to technological applications, principally in light emitting diodes (LEDs) [14] and solar cells [15,16] because of the wide band gap. So they have been studied in the form of bulk and thin film, due to a variety of their unique properties and potential applications. Cadmium sulfide is an important II–VI semiconductor with two different crystal structures: cubic zinc-blende with the space group F-43m, lattice parameter a = 5.87 Å, direct band gap of 2.48 eV and wurtzite hexagonal with the space group P63mc, lattice parameters a = 4.13, c = 6.75 Å, direct band gap of 2.5 eV [17, 18].

Cadmium sulfide was already successfully synthesized by various methods to obtain Bulk, thin film and nanoscale crystals [19, 20]. Some of these general preparation techniques were precipitation method, solvothermal and hydrothermal process, wet-chemical method, and etc. Mn doped CdS has attracted much attention owing to its properties that are closely related to the concentration of doping metal which caused the change of energy band and formed different luminescence centers [21-25]. So, in this work, undoped and Mn doped CdS nanoparticles grown by facile Chemical Co-precipitation method with two different ways and then investigate the effect of dopant concentration on the structure and properties of $Cd_{1-x}Mn_xS$ nanocrystals.

2. Experimental procedure

2.1. Materials and measurements

The involved samples were prepared using $Cd(Ac)_2.2H_2O$, $Mn(Ac)_2.2H_2O$, Na_2S, and Ethylene diamine tetraacetic (EDTA, EDTA acted as the capping agent) from Merck Ltd. All the chemicals and solvents employed for the synthesis were of analytical grade and used as received without further purification and deionized water were used in whole procedure.

The Fourier transform infrared (FTIR) analysis of the were recorded in the 4000–500 cm^{-1} wavelength region by using KBr disks as standard on a Thermo SCIENTIFIC model NICOLET iS10 spectrophotometer. X-ray powder diffraction (XRD) measurements were performed using a Philips X'pert diffractometer with monochromatic Cu-Kα radiation (λ = 1.54056 Å in a 2θ range of 10 - 70º in a continuous scan mode at scan Rate of 0.05 º/sec) to investigate the crystalline structure and phase identification. The UV-Vis absorption spectra were obtained by using a PG instruments Ltd, T70/T80 series (UV–Vis) spectrometer in the range of 800–200 nm wavelength. The nano samples were characterized by a scanning electron microscopy (SEM) (KYKY-EM3200). Ultrasonic generator was carried out on an ultrasonic bath wiseclean-wvc-A02H (frequency of 50 kHz).

2.2 Synthesis of CdS nanoparticles by co-precipitation method

The CdS nanoparticles were prepared as follows: 0.1 mol $Cd(Ac)_2.2H_2O$ and EDTA were dissolved in 50 ml of deionized water under continuous stirring, after that the desired amount of NH_4OH were used to adjust the PH of the solution to 7 to form clear liquid. In parallel, 0.1 mol Na_2S were added to 50 ml of deionized water. The Na_2S solution were then poured into $Cd(Ac)_2.2H2O$ and EDTA solution. After the reaction was completed, a yellow precipitate formed. Finally, this yellow precipitation was centrifuged at 300 prm for 30 min and then washed several times with absolute ethanol and deionized water to remove impurities. In order to characterization of CdS nanoparticles, this yellow precipitation was dried at 110 °C for 24 hours.

2.3 Synthesis of undoped and Mn doped CdS nanoparticles by co-precipitation method under ultrasonic irradiation

To study the effect of the ultrasonic irradiation on morphology and size of nanoparticles, the above processes were done under ultrasonic irradiation. After the SEM characterization, Mn doped CdS nanoparticles were prepared by co-precipitation method under ultrasonic irradiation.

Stoichiometric amounts of $Cd(Ac)_2.2H_2O$, $Mn(Ac)_2.2H_2O$ and EDTA was dissolved in 50 ml of deionized water. This solution was sonicated at room temperature until obtained a clear solution. In the next step, ammunia solution was added in this solution until PH reached at 7. Then 0.1 mol Na2S was dissolved in 50 ml of deionized water and added drop wise to the above solution under ultrasonic irradiation. The solution turned to yellow color immediately due to the formation of CdS nanoparticles. The solution was kept in the ultrasonic bath for a period of 30 min in order to complete the precipitation. The final precipitation was centrifuged at 300 prm for 30 min and then washed several times with absolute ethanol and deionized water to remove impurities and then dried at 110 °C for 24 hours.

3. Results and discussion

The structure, grain (crystalline) size and morphology of CdS sample prepared by only co-precipitation process and co-precipitation under ultrasonic irradiation were studied by X-ray diffraction (XRD) techniques and scanning electron microscopy (SEM). Fig. 1 presents the X-ray diffraction pattern of CdS sample (Fig. 1a) in comparison with the XRD pattern of this sample prepared by the sonochemical process (Fig. 1b).

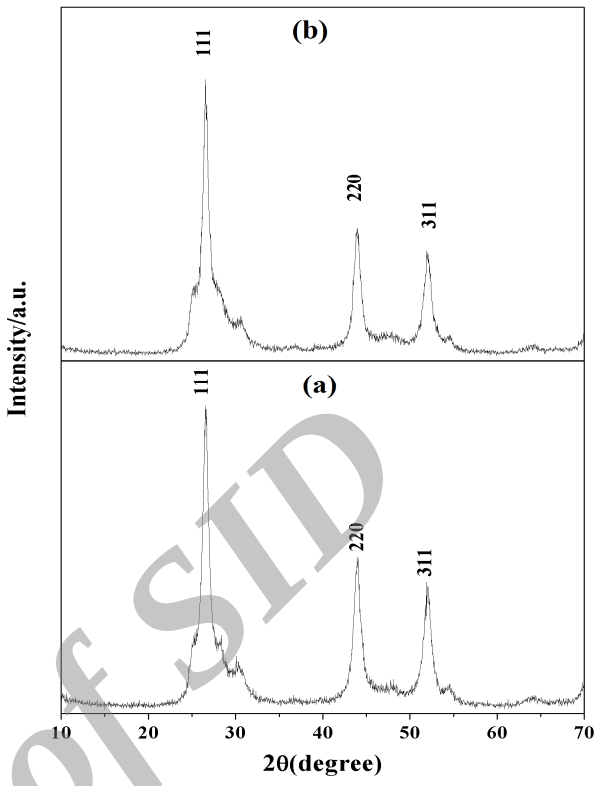

Fig. 1. XRD patterns of CdS nanoparticles synthesized by a) co-precipitation b) Ultrasound assisted co-precipitation method at room temperature

.

Acceptable matches, with slight differences in 2θ, were observed between these two experimental powder X-ray diffraction patterns. This indicates that sample obtained by these two processes as nanoparticles have identical structure and the significant broadening of the peaks indicates that the particles are of nanometer dimensions.

X-ray patterns analysis shows that the CdS samples crystallize in cubic symmetry with space group F-43M at room temperature, in agreement with the JCPDS No. 10-454. The lattice parameters are summarized in Table 1. It can be seen that, the three different XRD peaks of samples corresponding to the lattice planes of (111), (220) and (311) are very well consistent with the cubic

zinc-blended structure. This confirms the purity of the synthesized CdS samples.

Table 1. Cubic-cell lattice parameters of Cd1-xMnxS samples synthesized by co-precipitation method at room temperature.

composition (x)	a (Å)	V (Å^3)
0	5.806(9)	195.809(1)
0 (Ultrasound assisted)	5.813(2)	196.447(1)
0.1 (Ultrasound assisted)	5.806(3)	195.748(4)
0.2 (Ultrasound assisted)	5.803(2)	195.435(1)

The average particle size is approximately estimated by Hall's method [26]:

$$\frac{\beta\cos\theta}{\lambda}=\frac{1}{D}+\frac{2\varepsilon\sin\theta}{\lambda} \quad (1)$$

where β is the full width at half maximum (FWHM) of that peak in radian, θ is the diffraction angle of the Bragg peak, λ = 1.54056 Å is the wavelength of the used x-ray, D is the particle size, and ε is the effective residual strain. In this way, D can be estimated from the intercept on the $\beta\cos\theta/\lambda$ axis of the curve by plotting the $\beta\cos\theta/\lambda$ vs. $\sin\theta/\lambda$, respectively. An average particle size obtained in this way is about 10 nm (see Table 2).

Table 2. Energy band gap and calculated average particle size of Cd1-xMnxS samples synthesized by co-precipitation method at room temperature.

composition (x)	E_g (eV)	D_{XRD} (nm)	D_{UV} (nm)
0	-	12	-
0 (Ultrasound assisted)	3.28	7	1.7
0.1 (Ultrasound assisted)	3.47	9	1.6
0.2 (Ultrasound assisted)	3.32	9	1.7

Fig. 2a and 2b present SEM images of CdS samples with different synthesized process. Comparison between these samples shows different results.

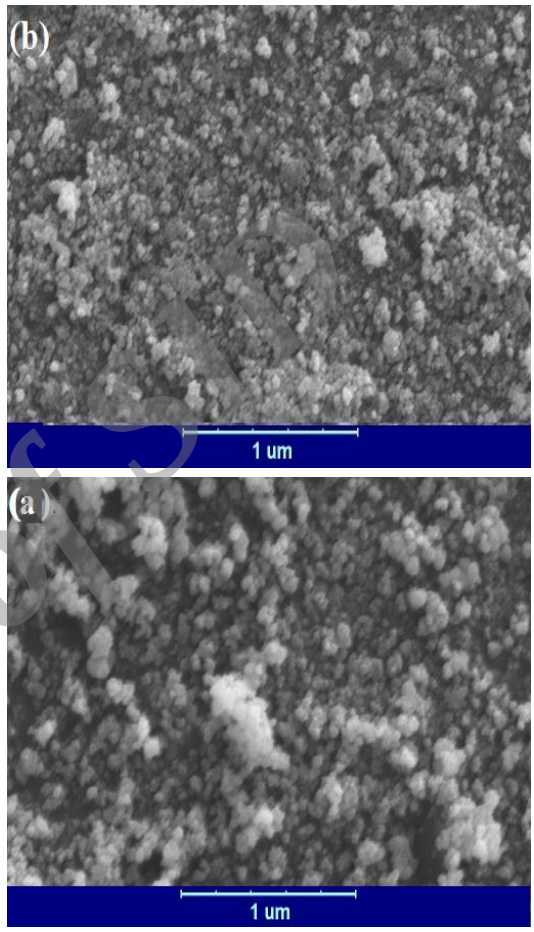

Fig. 2. Scanning electron images of CdS nanoparticles synthesized by a) co-precipitation b) Ultrasound assisted co-precipitation method.

As it has been seen in Fig. 2a, co-precipitation method without ultrasonic irradiation is yielded more agglomerated particles with the mean size of about 40 nm. At ultrasonic irradiation, it seems the size of particles is decreased and lower agglomeration of particles was happened. One can see (in Fig. 2b) polyhedral but nearly spherical nanoparticles posing an almost homogenous size

distribution with the mean size of 10-20 nm, comparable with the value obtained from the broadening of XRD peaks. Therefore, it can be concluded that ultrasonic irradiation avoids agglomeration of particles. So the sonochemical process has been considered as the optimized synthesized process and the morphology and particle size of the nanostructures depend on condition of synthesized process.

Fig. 3 presents XRD patterns for the $Cd_{1-x}Mn_xS$ (x = 0, 0.1, 0.2) samples at 300 K. A satisfactory accordance of these X-ray diffraction patterns can be seen. The lattice parameters are summarized in Table 1. The XRD patterns show that all samples in the studied composition range are highly single phase and also crystallize in cubic symmetry with space group F-43M. It can be seen that, although the structure does not undergo any change on partial replacement of Cd by Mn, there is a slight reduction of lattice parameters and the cell volume as the Mn content increases. This is related to the smaller ionic radii of Mn ion (r_{Cd2+} = 0.92 Å and r_{Mn2+} = 0.80 Å) (see Table 1). The crystallite size of all samples is also estimated from the full width at half maximum (FWHM) of the characteristic XRD peaks using Hall's method (Eq. 1).

SEM images of $Cd_{1-x}Mn_xS$ (x = 0, 0.1, 0.2) are presented in Fig 4. Particle size of the nanostructures depends on the concentration of dopant. Comparison between the samples with different concentrations shows that an almost reduction of concentrations decreases the particles size and also leads to uniform nanoparticles morphology. Thus, samples produced using lower concentrations of dopant (Fig. 4a) have smaller particle size than the ones with higher concentrations (Fig. 4c).

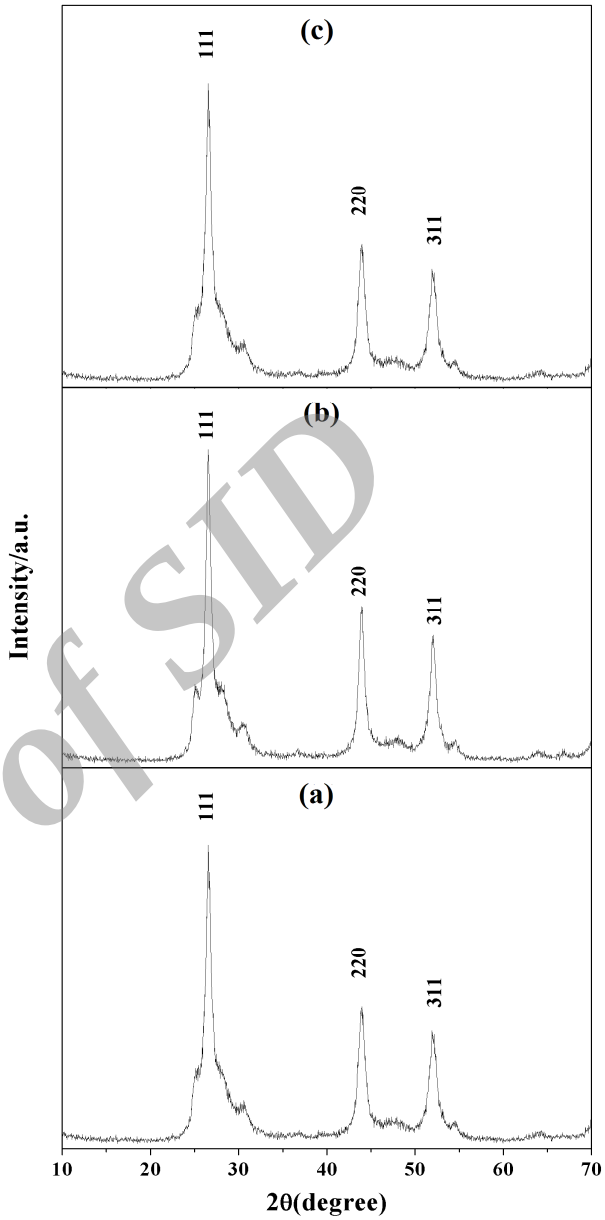

Fig. 3. XRD patterns of $Cd_{1-x}Mn_xS$ a) x = 0, b) x = 0.1 and c) x = 0.2 nanoparticles synthesized by Ultrasound assisted co-precipitation method at room temperature.

SEM images of $Cd_{1-x}Mn_xS$ (x = 0, 0.1, 0.2) are presented in Fig 4. Particle size of the nanostructures depends on the concentration of dopant. Comparison between the samples with different concentrations shows that an almost reduction of concentrations decreases the particles size and also leads to uniform nanoparticles

morphology. Thus, samples produced using lower concentrations of dopant (Fig. 4a) have smaller particle size than the ones with higher concentrations (Fig. 4c).

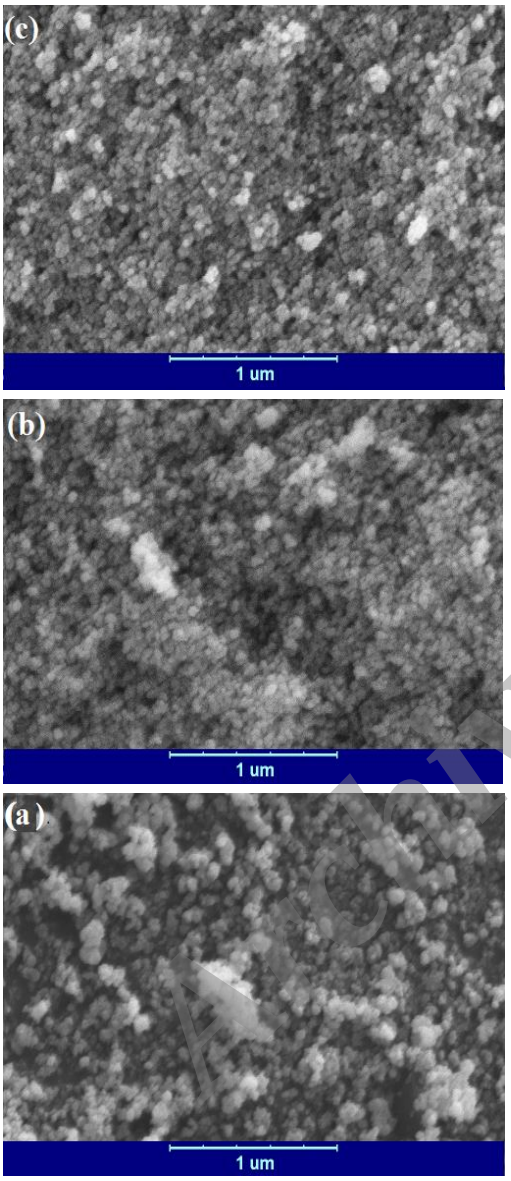

Fig. 4. Scanning electron images of $Cd_{1-x}Mn_xS$ a) x = 0, b) x = 0.1 and c) x = 0.2 nanoparticles synthesized by Ultrasound assisted co-precipitation method at room temperature.

The FTIR spectra of $Cd_{1-x}Mn_xS$ (x = 0, 0.1, 0.2) nanoparticles at room temperature are shown in Fig. 5. This spectrum is showing IR absorption due to the various vibration modes. The observed peaks at 1600-1620 cm^{-1} are attributed to the C=O stretching modes and also the broad absorption band in the range of 3420-3480 cm^{-1} attesting the presence of O-H stretching modes arising from the absorption of water on the surface of nanoparticles via -COOH group [27]. The peaks of CdS can be observed at about 1136, 1007 and 668 cm^{-1}. The peak of about 668 cm^{-1} is nearly unchanged upon doping which is assigned to the characteristic major peaks of CdS, in good agreement with the reported literature [28], and the other two peaks join with each other may be ascribed to the Zn-Mn vibration.

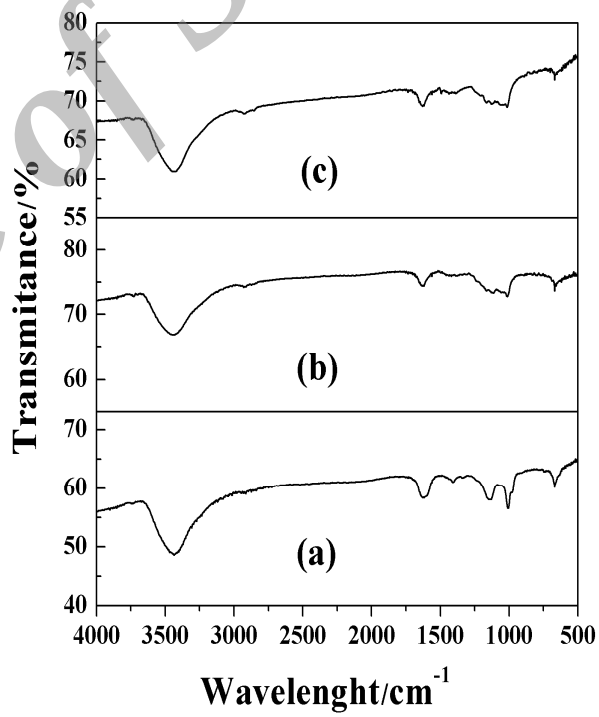

Fig. 5. FTIR spectra of $Cd_{1-x}Mn_xS$ a) x = 0, b) x = 0.1 and c) x = 0.2 nanoparticles synthesized by Ultrasound assisted co-precipitation method.

The room temperature UV-Vis spectra of $Cd_{1-x}Mn_xS$ (x = 0, 0.1, 0.2) nanoparticles in the absorption mode are presented in Fig. 6. As seen, the presence of a band gap is indicated by a nearly

sudden decrease in the absorbance at a particular wavelength.

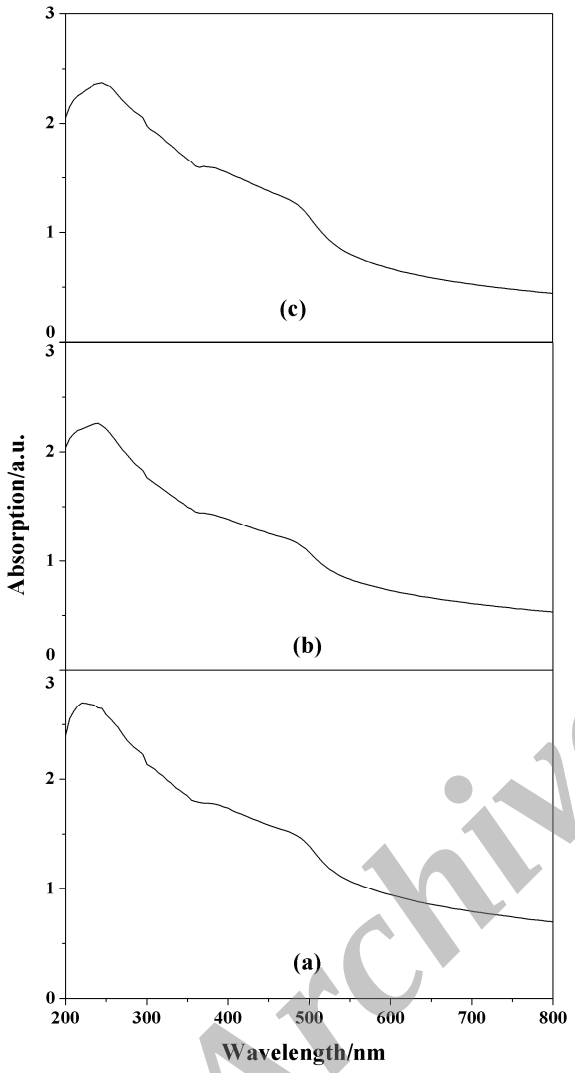

Fig. 6. UV-Vis spectra of $Cd_{1-x}Mn_xS$ a) x = 0, b) x = 0.1 and c) x = 0.2 nanoparticles synthesized by Ultrasound assisted co-precipitation method.

The optical band gap of these nanoparticles calculated from the UV absorption study corresponds to the electronic transitions assigned to intervalence charge transference. Further, for the determination of optical band gap, we have plotted the Tauc function (Eq. 2) with the energy (Fig. 7) [29].

$$\alpha h\nu = A(h\nu - E_g^{opt})^n \quad (2)$$

where α is the absorption coefficient, hν is the incident photon energy, A is a constant, and E_g^{opt} is the optical band gap energy of the material

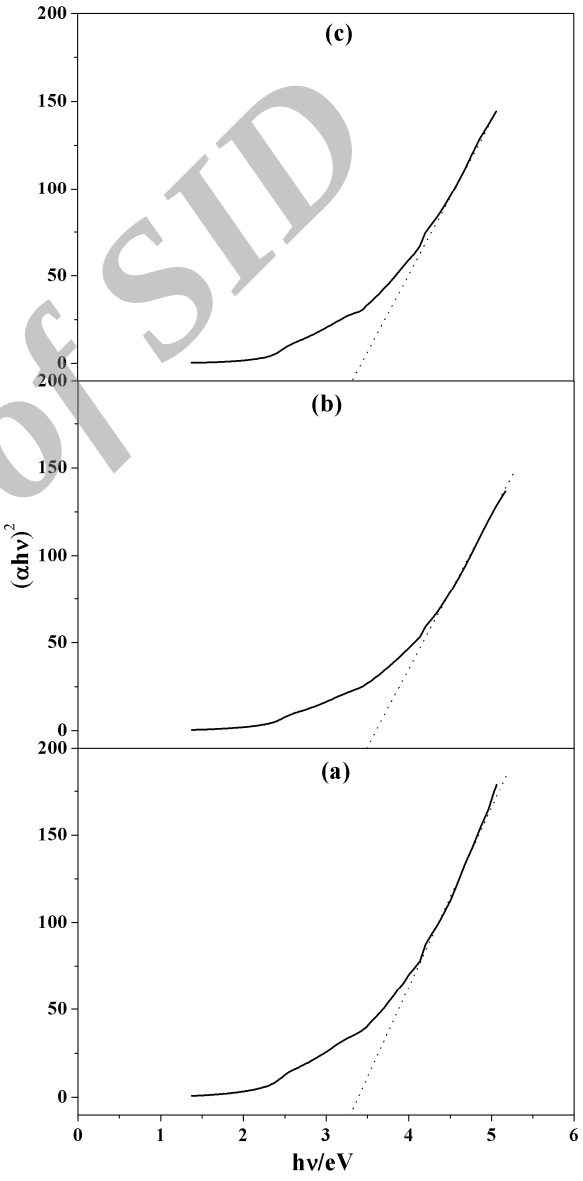

Fig. 7. Determination of Optical band gap of $Cd_{1-x}Mn_xS$ a) x = 0, b) x = 0.1 and c) x = 0.2 nanoparticles synthesized by Ultrasound assisted co-precipitation method.

The value of the exponent depends on the type of transition: 1/2 for allowed direct transition and 2 for allowed indirect transition. The optical band gap of $Cd_{1-x}Mn_xS$ nanoparticles is determined by plotting $(\alpha hv)^2$ vs. hν and extrapolating the straight line portion of $(\alpha hv)^2$ to $(\alpha hv)^2 = 0$ (Fig. 7).

The band gap of nanoscale materials is mainly associated with two factors: quantum size effects (as the particle size decreases there is increase in effective band gap due to confinement of charge carriers in a very small dimension) and surface and interface effects [30]. The quantum size effect causes the blue shift or increasing band gap while the surface and interface effects leads to the red shift or decreasing band gap by decreasing particle size [30,31]. The value of the optical band gap energy of CdS sample is found to be 3.28 eV. A comparison with the value of 2.48 eV for bulk CdS [17,18] shows that the band gap is blue-shifted which is in accordance with the quantum size effects of the photogenerated electron-hole pairs. From optical absorption spectra it is found that Mn concentration does not influence to the absorption spectra.

It is known that the particle size is also calculated from the absorption values using the effective mass approximation relation [32]:

$$E_g^{opt} = E_g + \frac{\hbar^2\pi^2}{2r^2}\left(\frac{1}{m_e^*}+\frac{1}{m_h^*}\right) - \frac{1.786e^2}{\varepsilon r} - \frac{0.124e^2}{\hbar^2\varepsilon^2}\left(\frac{1}{m_e^*}+\frac{1}{m_h^*}\right)^{-1} \quad (3)$$

where E_g^{opt} and E_g is the calculated optical band gap of the nanoparticles and the bulk band gap (CdS=2.48 eV), respectively, r is the radius of the nanoparticle in meter, m_e^* and m_h^* is electron and hole effective mass, e is the charge of the electron and ε is the dielectric constant (CdS=8.9). The value of the effective mass of electrons and holes for CdS is $m_e^* = 0.54\ m_e$ and $m_h^* = 0.21\ m_h$. The second and third terms are much smaller than the first term [33], therefore may be neglected and the expression reduces to

$$r = \frac{1.5606}{\left(E_g^{opt} - E_g\right)^{\frac{1}{2}}} \quad (4)$$

The calculated particles size is about 2 nm that is in agreement with the size estimated from the XRD result, approximately. The energy band gap and particles size of the samples are summarized in Table 2.

4. Conclusion

Nanosized $Cd_{1-x}Mn_xS$ (x = 0, 0.1, 0.2) samples were synthesized by only co-precipitation and ultrasound assisted co-precipitation method compared with its crystalline structure and size of particles. Results show that the morphology and size of nanoparticles depend on ultrasound irradiation and the appropriate nanosized samples were obtained by ultrasound assisted co-precipitation method. SEM images reveal that Cd1-xMnxS nanoparticles have almost regular shapes with an average size of 10-20 nm. The physical properties are affected due to the quantum size effect. Mn substitution causes no structural transition and all samples crystallized in cubic symmetry with a space group of F-4m. However, due to the smaller ionic size of Mn ions, a reduction in cell volume is observed. The enhancement of band gap is attributed to the quantum size effects due to decreasing particle size.

References

[1] A. P. Alivisatos, Science 271 (1996) 933-937.

[2] J. R. Heath, Ed. Acc. Chem. Res. 32(1999) 389-396.

[3] Q. Wang, G. Xu, G. Han, J. Solid State Chem. 178 (2005) 2680-2685.

[4] H. M. Fan, X. F. Fan, Z. H. Ni, Z. X. Shen, Y. P. Feng, B. S. Zou, J Phys Chem C 112 (2008) 1865-1870.

[5] Q. Nie, Q. Yuan, W. Chen, J. Cryst. Growth 265 (2004) 420-424.

[6] X. Ma, F. Xu, Z. Zhang, Mater. Res. Bull. 40 (2005) 2180-2188.

[7] Y. Wang, C.Y. To, D.H.L. Ng, Mater. Lett. 60 (2006) 1151-1155.

[8] R. Romano, O. L. Alves, Mater. Res. Bull. 41 (2006) 376-386.

[9] Y. Yang, H. Chen, X. Bao, J. Cryst. Growth. 252 (2003) 251- 256.

[10] A. Kassis, M. Saad, Solar Energy Materials and Solar Cells 80 (2003) 491-499.

[11] C. Yang, X. Zhou, L. Wang, X. Tian, Y. Wang, Z. Pi, J.Mater.Sci. 44 (2009) 3015-3019.

[12] P.Y. Yu, M. Cardona, Fundamentals of semiconductors, Springer-Verlag (1983).

[13] S.V. Gaponenko, Optical properties of semiconductor nanocrystals, Cambridge University Press (2005).

[14] M.C. Schlamp, X. Peng, A.P. Alivisatos, J. Appl. Phys. 82 (1997) 5837-5842.

[15] Y. Shen, Y. Lee, Nanotechnology 19 (2008) 045602- 045608.

[16] S. Biswas, M.F. Hossain, T. Takahashi, Thin Solid Films 517 (2008) 1284-1288.

[17] T. Suzuki, T. Yagi, S. Akimoto, T. Kowamura, S. Tayoda, S. Endo, J. Appl. Phys. 54 (1983) 748-760.

[18] A.N. Mariano, E.P. Warekois,Science 142 (1963) 672-673.

[19] S. Prabahar, N. Suryanarayanan, D. Kathirvel, Chalcogenide Letters 6 (2009) 577-581.

[20] M.J. Pawar, S.S. Chaure, Chalcogenide Letters 6 (2009) 689-693.

[21] A. Ishizumi, K. Matsuda, T. Saiki, C.W. White, Y. Kanemitsu, Appl. Phys. Lett. 87 (2009) 1331040- 1331043.

[22] A. Nag, S. Sapra, C. Nagamani, A. Sharma, N. Pradhan, S.V. Bhat, D.D. Sarma, Chem. Mater. 19 (2007) 3252-3259.

[23] A. Nag, S. Sapra, S.S. Gupta, A. Prakash, A. Ghangrekar, N. Periasamy, D.D. Sarma, Bull. Mater. Sci. 31 (2008) 561-568.

[24] C.W. Na, D.S. Han, D.S. Kim, Y.J. Kang, J.Y. Lee, J. Park, D.K. Oh, K.S. Kim, D. Kim, J. Phys. Chem. B 110 (2006) 6699-6704.

[25] D.S. Kim, Y.J. Cho, J. Park, J. Yoon, Y. Jo, M.H. Jung, J. Phys. Chem. C 111 (2007) 10861-10868.

[26] J. Hasanzadeh, A. Taherkhani, M. Ghorbani, Chinese Journal of Physics 51 (2013) 540-550.

[27] K. Nakamoto,Infrared and Raman Spectra of Inorganic and Coordination Compounds, 5 ed. New York, John Wiley (1997).

[28] B.R. Singh, S. Dwivedi, A.A. Al-Khedhairy, J. Musarrat, Colloids and Surfaces B: Biointerfaces (2011) 207–213.

[29] B. Srinivasa Rao, B. Rajesh Kumar, V. Rajagopal Reddy, T. Subba Rao, Chalcogenide Letters 8 (2011) 177-185.

[30] P. Kumar, H.K. Mali, A. Ghosh, R. Thanavel, K. Asokan, Appl. Phys. Lett. 102 (2013) 221903- 221908.

[31] Z.H. Yuan, W. You, J.H. Jia, L.d. Zhang, Chin. Phys. Lett. 15 (1998) 535-536.

[32] J.P. Borah, K.C. Sarma, ACTA PHYSICA POLONICA A 114 (2008) 713-719.